Science Advances
AAAS

advances.sciencemag.org/cgi/content/full/6/22/eaba3167/DC1

Supplementary Materials for

Monocyte-derived multipotent cell delivered programmed therapeutics to reverse idiopathic pulmonary fibrosis

Xin Chang, Lei Xing, Yi Wang, Chen-Xi Yang, Yu-Jing He, Tian-Jiao Zhou, Xiang-Dong Gao, Ling Li, Hai-Ping Hao*, Hu-Lin Jiang*

*Corresponding author. Email: hhp_770505@hotmail.com (H.-P.H.); jianghulin3@gmail.com (H.-L.J.)

Published 27 May 2020, *Sci. Adv.* **6**, eaba3167 (2020)
DOI: 10.1126/sciadv.aba3167

This PDF file includes:

Figs. S1 to S10

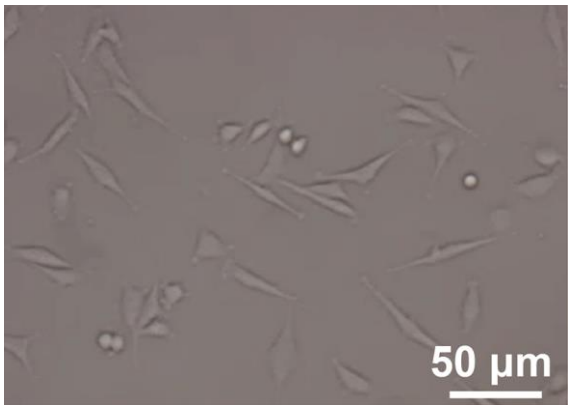

Fig. S1. The morphologies of MOMC. The morphology of the MOMC was fusiform.

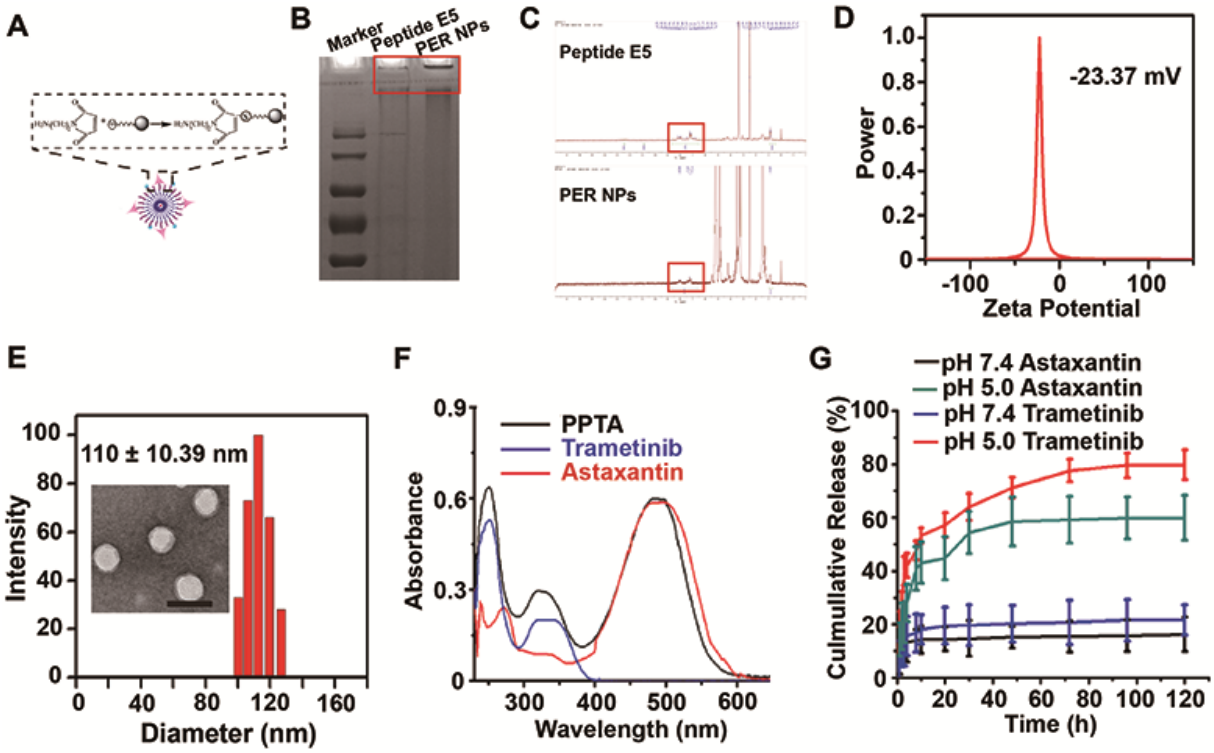

Fig. S2. The physical-chemical characterization of PER NPs. (**A**) The schematic for modification of peptide E5. (**B**) The modification results by SDS-PAGE and (**C**) ^{1}H NMR spectroscopy. (**D**) ζ-potential of PER NPs by Brookhaven Instruments. (**E**) Particle-sizes distribution and morphologies of PER NPs by Brookhaven Instruments and TEM, respectively. Scale bar: 100 nm. (**F**) The UV-vis absorption of TRA, AST and PPTA. (**G**) The release profiles of AST and TRA at pH 5.0 and pH 7.4.

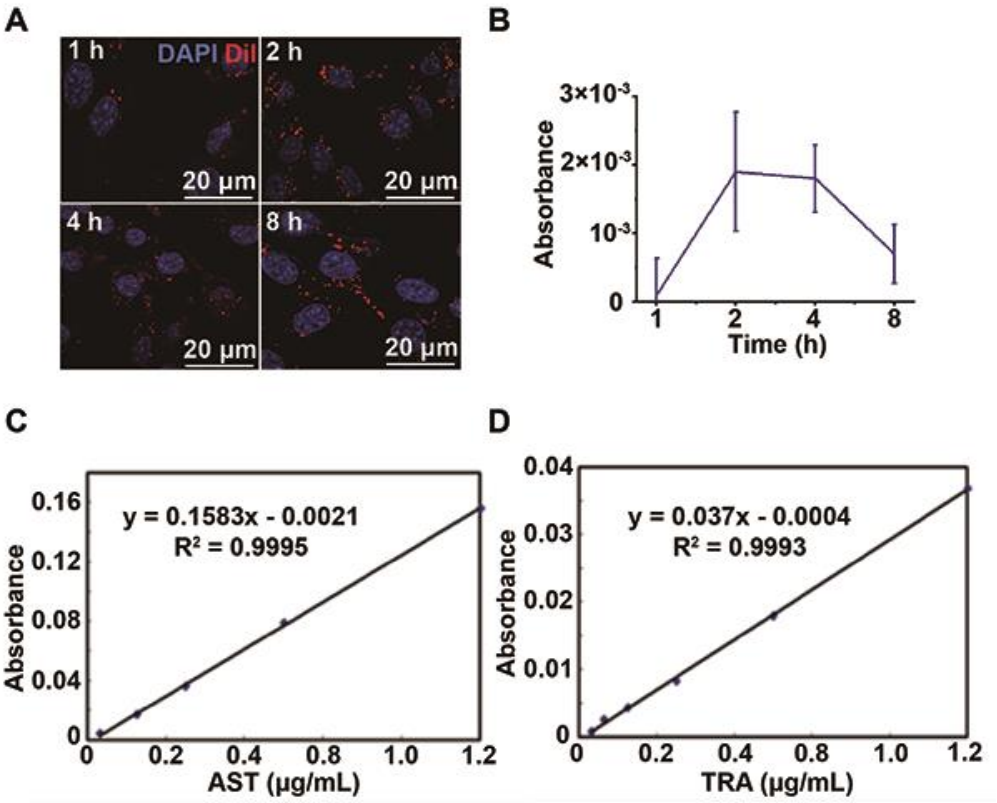

Fig. S3. The loading ability of MOMC. The loading ability of MOMC was detected by confocal images (**A**) and spectrophotometer (**B**). Standard curves of AST (**C**) and TRA (**D**).

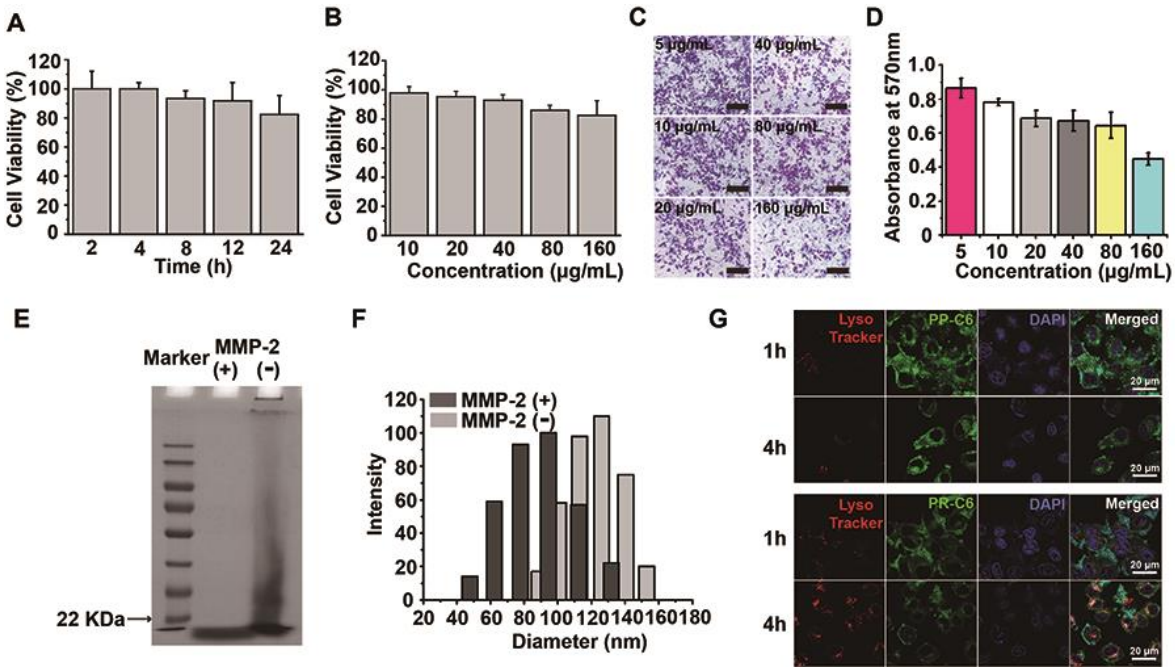

Fig. S4. The characterization of interaction of MOMC and PER NPs. Potential toxicity of PER NPs for MOMC after incubated at different time points (**A**) and concentration (**B**). (**C** and **D**) The migration assay of MOMC was investigated after loading with different concentrations of PER NPs by CXCR 4 receptor and CXCL 12 (n = 3), scale bar: 100 μm. The released capacity of PER NPs from MOMC was detected *via* MMP-2 enzyme by SDS-PAGE (**E**) and DLS (**F**), respectively. (**G**) The lysosomes escape capability of PP-C6 and PR-C6 was investigated by CLSM, scale bar: 20 μm.

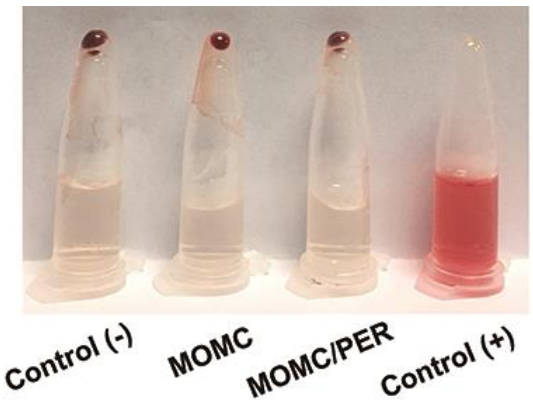

Fig. S5. Hemolysis test. The hemolysis test of MOMC and MOMC/PER *in vivo*. Photo Credit (Fig. S5): Xin Chang, China Pharmaceutical University;

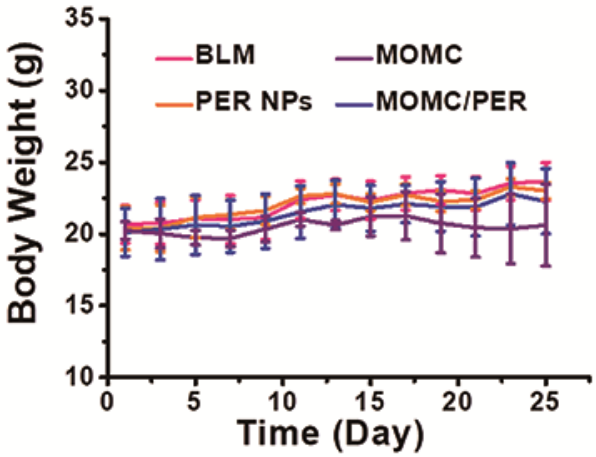

Fig. S6. Body weight. The changes of body weight in the process of treatment in different formulations (n = 5).

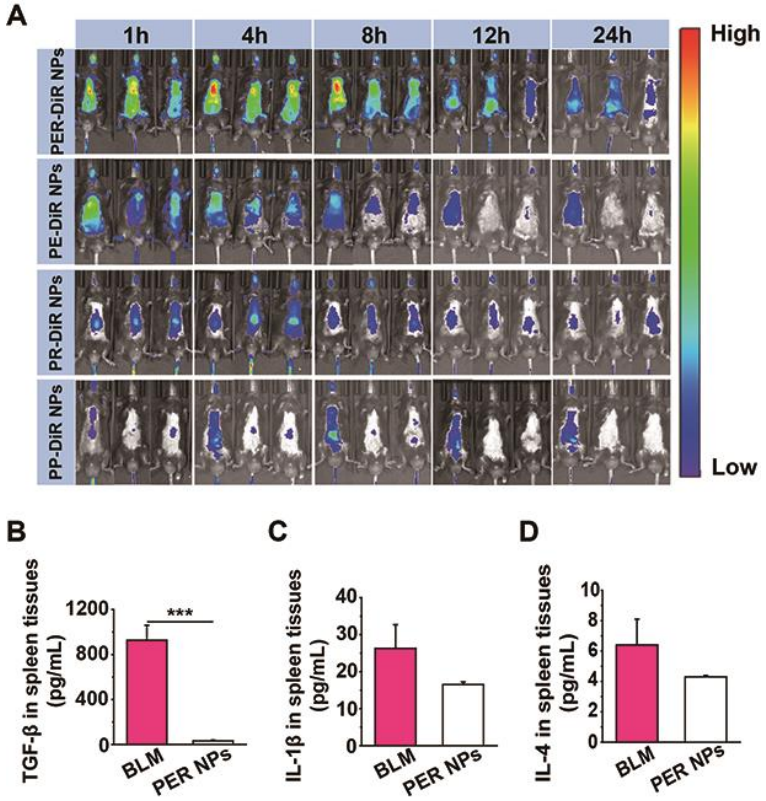

Fig. S7. The targeting ability and therapeutic efficacy of PER NPs *in vivo*. (**A**) The targeting ability in each group using IVIS living system (n = 3). The levels of TGF-β (**B**), IL-1β (**C**) and IL-4 (**D**) were detected by ELISA assay in spleen tissues after treatments (n = 5). Statistical significance was calculated *via* one-way analysis of variance (ANOVA).

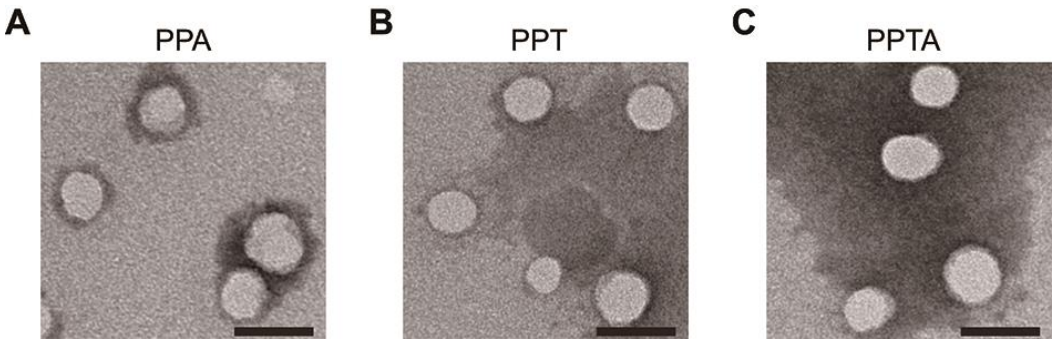

Fig. S8. The TEM images of PPA, PPT, PPTA. (**A**) The morphologies of PPA. (**B**) The morphologies of PPT. (**C**) The morphologies of PPTA. Scale bars: 100 nm.

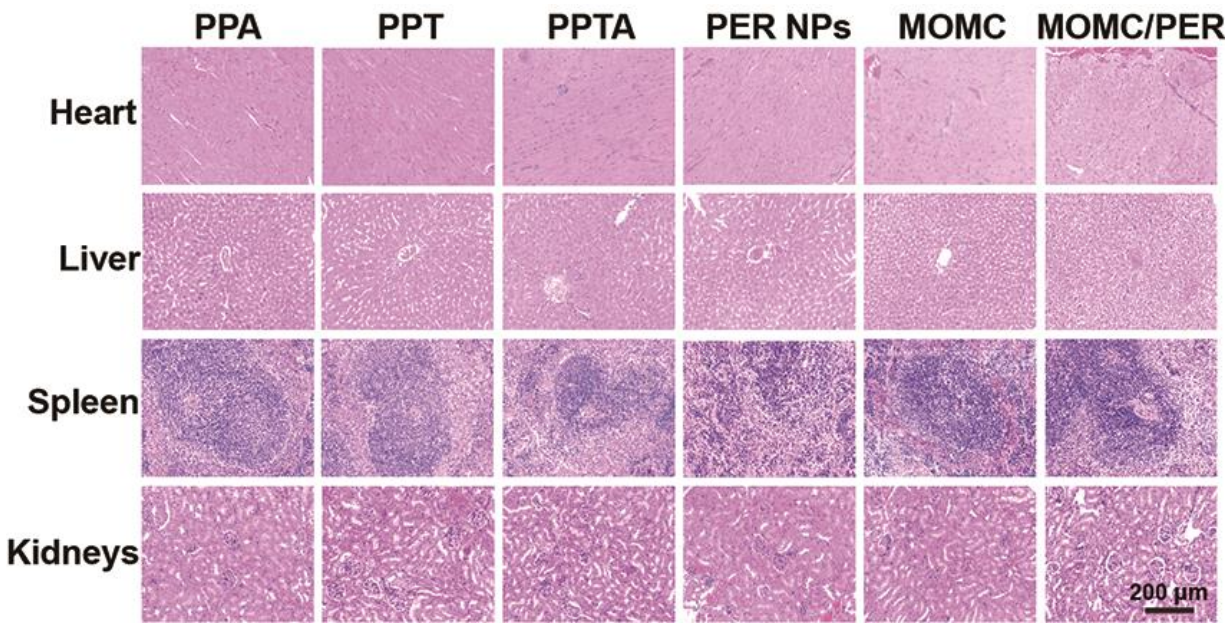

Fig. S9. Systemic toxicity after treated with different formulations. The potential toxicity in each organ after treated with different treatments.

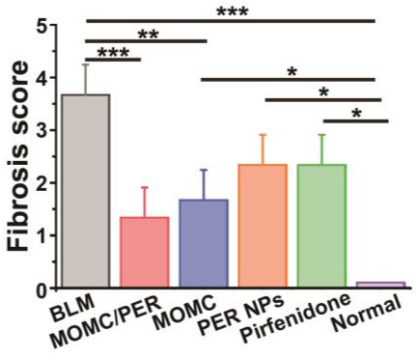

Fig. S10. The fibrosis score of different formulations in lung tissues (n = 3). Statistical significance was calculated *via* one-way analysis of variance (ANOVA).